Neuroradiology (1997) 39: 258–264

R. A. Bhadelia
A. R. Bogdan
R. F. Kaplan
S. M. Wolpert

Cerebrospinal fluid pulsation amplitude and its quantitative relationship to cerebral blood flow pulsations: a phase-contrast MR flow imaging study

Received: 3 January 1996
Accepted: 5 June 1996

R. A. Bhadelia (✉) · S. M. Wolpert
Section of Neuroradiology,
Department of Radiology,
New England Medical Center Hospitals
and Tufts University,
750 Washington Street, Boston,
MA 02111, USA

A. R. Bogdan
Department of Radiation Oncology,
New England Medical Center Hospitals
and Tufts University,
750 Washington Street, Boston,
Massachusetts, USA

R. F. Kaplan
Department of Neurology,
New England Medical Center Hospitals
and Tufts University,
750 Washington Street, Boston,
Massachusetts, USA

Abstract Our purpose in this investigation was to explain the heterogeneity in the cerebrospinal fluid (CSF) flow pulsation amplitudes. To this end, we determined the contributions of the cerebral arterial and jugular venous flow pulsations to the amplitude of the CSF pulsation. We examined 21 healthy subjects by cine phase-contrast MRI at the C2–3 disc level to demonstrate the CSF and vascular flows as waveforms. Multiple regression analysis was performed to calculate the contributions of (a) the arterial and venous waveform amplitudes and (b) the delay between the maximum systolic slopes of the arterial and venous waveforms (AV delay), in order to predict the amplitude of the CSF waveform. The contribution of the arterial waveform amplitude was positive ($r = 0.61$; $p = 0.003$) to the CSF waveform amplitude and that of the venous waveform amplitude was negative ($r = –0.50$; $p = 0.006$). Both in combination accounted for 56 % of the variance in predicting the CSF waveform amplitude ($p < 0.0006$). The contribution of AV delay was not significant. The results show that the variance in the CSF flow pulsation amplitudes can be explained by concurrent evaluation of the CSF and vascular flows. Improvement in the techniques, and controlled experiments, may allow use of CSF flow pulsation amplitudes for clinical applications in the non-invasive assessment of intracranial dynamics by MRI.

Key words Magnetic resonance imaging · Cerebrospinal fluid dynamics · Cerebral blood flow · Physiology

Introduction

Cardiac cycle-related cerebral blood volume variations produce bi-directional oscillatory movement of cerebrospinal fluid (CSF) within the craniospinal axis [1–15]. During systole, net inflow of blood increases the intracranial volume and induces craniocaudal (systolic) CSF flow. During diastole, net outflow of blood decreases the intracranial volume and promotes caudocranial (diastolic) CSF flow. Phase-contrast MRI noninvasively displays this pulsatory CSF motion and allows assessment of its amplitude [3–15]. Nevertheless, the clinical utility of the CSF flow amplitude analysis has remained limited due to a wide variation in normal subjects [12, 15].

It has been proposed that the amplitude of the CSF pulsation depends on the amounts of the cerebral arterial inflow and venous outflow and on the temporal delay between the two flows [16, 17]. Although phase-contrast MRI has been used to demonstrate the temporal relationship between the CSF and the vascular flow pulsations [5, 8, 10–12, 14], to our knowledge, the quantitative relationship between the CSF pulsation amplitudes and the vascular flow pulsations has not been examined. We sought to show in healthy subjects, the CSF as well as the cerebral arterial and jugular venous flow pulsations as waveforms by phase-contrast MRI, and to assess the contributions of the vascular waveform amplitudes to the CSF waveform amplitudes. The contri-

bution of the temporal delay measured between the maximum systolic slopes of the arterial and venous waveforms to the CSF waveform amplitude was also determined [14]. For the arterial waveform the maximum systolic slope represents maximum rate of change (acceleration) in the cranial flow, and for the venous waveform it represents maximum rate of change in the caudal flow. Therefore, the arteriovenous (AV) delay measured between these points in the cardiac cycle is likely to reflect a time during which maximal systolic expansion is taking place in the cerebral blood volume.

Methods

The CSF and vascular flows at the C2–3 disc level were examined in 21 healthy subjects by cine phase-contrast MRI on a 1.5-T unit. There were 11 women and 10 men aged 24–45 years (mean: 34 years). The arterial blood pressures measured prior to the experiments were normal in all subjects.

A commercially available retrospectively cardiac-gated cine phase-contrast (cine PC) sequence was used [12, 14]. Modification of the post-processing algorithm allowed reconstruction of true phase images with pixel value reading in units of 0.1 mm/s [14, 18]. A repetition time of 50 ms was used throughout the study, providing a temporal resolution of approximately 100 ms [9, 14, 15, 18]. In order to obtain optimal temporal information in subjects with different heart rates, the number of radiofrequency pulses (reconstructed images) were varied between 16 and 24 (a higher number of images were reconstructed for subjects with slow heart rate). Peripheral pulse triggering was used for the detection of the R-wave of the ECG.

The following flow studies were performed at the C2–3 disc level in each subject after obtaining a sagittal T1-weighted localizer (500/20; TR/TE):

1. Axial CSF flow study of the cervical subarachnoid spaces.

2. Axial vascular flow study of the internal carotid and vertebral arteries, and the internal jugular veins. A localizer gradient-echo sequence was used to ensure that the vessels were perpendicular to the scan plane.

The technical factors for the flow experiments were: (1) CSF flow study: 50/15/2 (repetition time/echo time/excitations), 15 deg flip angle, 18 cm field of view, and velocity encoding (Venc) 5–7 cm/s; and (2) vascular flow study: 50/10/1, 30 deg flip angle, 20 cm field of view, and Venc 60–80 cm/s. In addition, a 256×192 matrix and 3 mm slice thickness were used. The direction of flow encoding was superior-to-inferior for both studies.

The images were transferred to a SPARC station 10. Computer programs were developed using PV-Wave Advantage software to determine the CSF and vascular waveforms by plotting flow rates on the Y-axis and fractions of the cardiac cycle on the X-axis.

Volume flow rates (in ml per min) were calculated for each image by multiplying the average signal intensity (average velocity) of a defined region of interest (ROI) with its area [12]. The signal intensity values were adjusted for eddy current-induced additive errors by background subtractions [12, 14, 18]. The C2–3 CSF flow area was determined by subtracting the traced area of the spinal cord from that of the thecal sac (Fig. 1 a). The arterial flow area was determined by tracing the outlines of the internal carotid and vertebral arteries, and the venous flow area was determined by tracing the outlines of both internal jugular veins (Fig. 1 b). The cerebral arterial flow rate represented the sum of the internal carotid and vertebral arteries. The jugular venous flow rate represented the sum of both internal jugular veins.

The amplitudes of the CSF flow waveforms were defined as the difference between the maximum systolic (craniocaudal) CSF flow rate and the maximum diastolic (caudocranial) CSF flow rate (Fig. 2). The amplitudes of the vascular flow waveforms were defined as the difference between the maximum and the minimum flow rates (Fig. 3).

Slopes were calculated at each time point on the arterial and venous flow waveforms, and were viewed along with the vascular waveforms [14]. The intervals between the R-wave and the maximum systolic slope (R-MSS) on the arterial and venous waveforms were determined (Fig. 3). The AV delay was determined by subtracting the R-wave to the maximum systolic slope interval of the arterial waveform from that of the venous waveform.

The average, range and standard deviation values were determined for the CSF, arterial and venous flow waveform amplitudes, for the R-wave to the maximum systolic slope intervals of the arterial and venous waveforms, and for the AV delays. Stepwise forward multiple regression was used to calculate the contributions of the arterial and venous flow waveform amplitudes and of the AV delay in predicting the CSF flow waveform amplitude.

Results

The amplitudes of the CSF and vascular flow waveforms, the R-wave to the maximum systolic slope intervals of the vascular flow waveforms and the durations of the AV delays are indicated in Table 1. Note that the CSF and the vascular waveform amplitudes show considerable variability. The R-wave to the maximal systolic slope interval of the arterial waveform was less variable than that of the jugular venous waveform. Considerable variability was seen in the AV delay data.

Table 2 shows the results of stepwise forward multiple regression. A significant positive correlation was observed between the CSF and arterial waveform amplitudes; subjects with large arterial amplitudes showed large CSF flow waveform amplitudes. A significant negative correlation was observed between the CSF and the jugular venous waveform amplitudes; subjects with large venous waveform amplitudes had small CSF flow waveform amplitudes. The AV delay showed a weak positive correlation with the CSF waveform amplitude which was not significant.

Both the arterial and the venous waveform amplitudes contributed significantly to predicting the CSF waveform amplitudes. Each contributed independently, and in combination they accounted for over 56 % of the variance seen in the CSF waveform amplitude ($p = 0.0006$). The contribution of the AV delay did not significantly add to predicting the CSF flow waveform amplitude, suggesting that this variable's contribution is not independent.

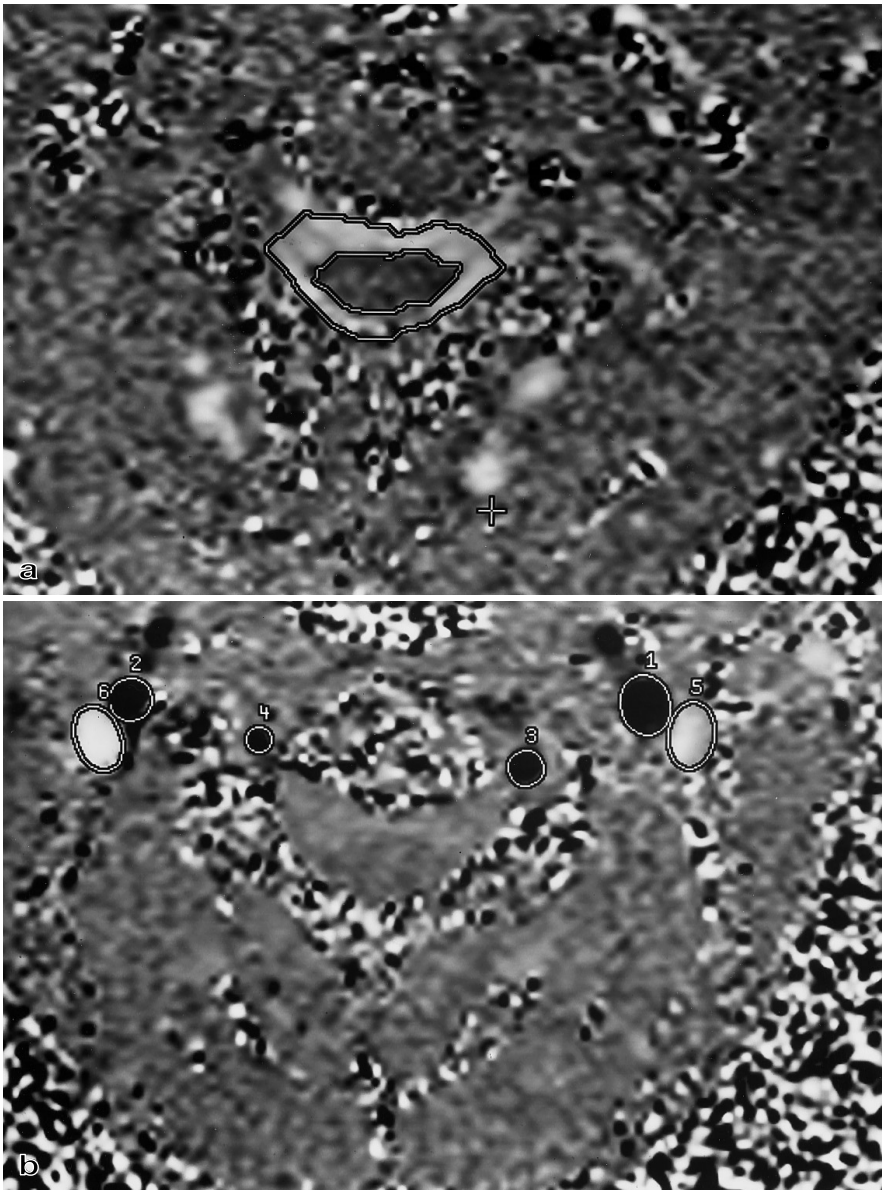

Fig. 1 a, b Axial cine phase-contrast studies at the C2–3 disc level. **a** CSF flow study: the outlines of the thecal sac and the spinal cord are traced to obtain the CSF flow area. **b** Vascular flow study: the outlines of the internal carotid and vertebral arteries and both internal jugular veins are traced

Discussion

The Monro-Kellie doctrine assumes that the volume of the contents of the cranial cavity, consisting of brain, blood and CSF, remains constant [8, 19, 20]. Accordingly, any increase or decrease in the volume of one of these components necessitate a reciprocal change in the volume of the remaining components. Both blood and CSF can rapidly flow in and out of the cranial cavity, and therefore provide swift compensation for alterations in the intracranial volume associated with the cardiac cycle [21]. Net inflow of arterial blood during cardiac systole increases the intracranial volume and is compensated by immediate venous egress and systolic (craniocaudal) CSF displacement to the spinal canal [2, 11–14]. Net outflow of blood during diastole decreases the intracranial volume and promotes the diastolic (caudocranial) CSF displacement from the spinal canal into the cranium [13, 18]. Thus, a larger systolic inflow of blood exerts a greater burden on this compensatory mechanism and requires both increased venous egress and systolic CSF displacement as compared to a smaller systolic inflow of blood. If the venous egress can effectively increase, to handle this extra volume of arterial inflow, only a small increase in the systolic CSF displacement may result. However, if a rapid increase in the venous egress does not ensue, a large systolic CSF displacement may occur [21]. The positive relationship between the

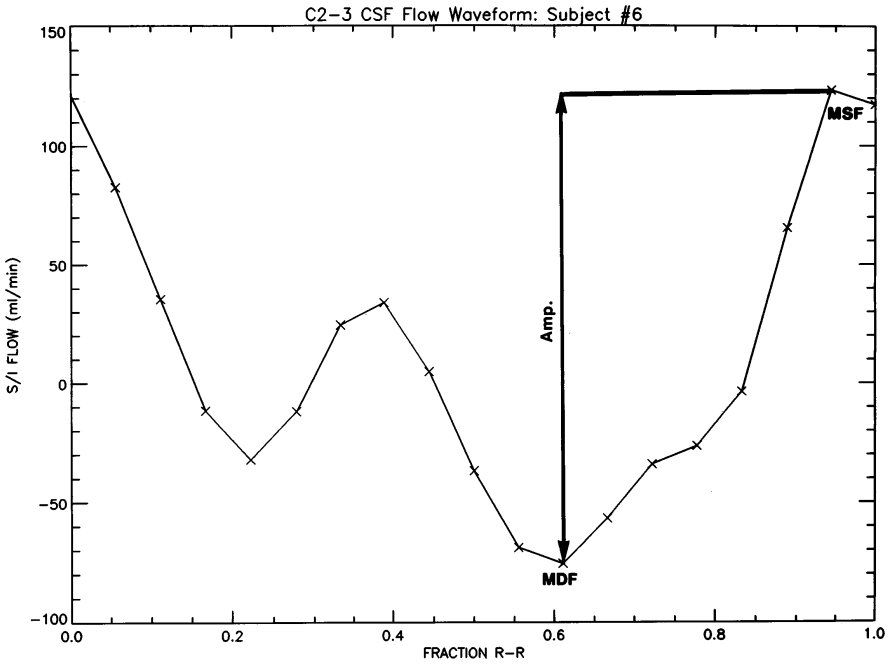

Fig. 2 CSF flow waveform. Fractions of cardiac cycle on X-axis and flow rates in ml/min on Y-axis. Positive deflections represent systolic (craniocaudal) CSF flow and negative deflections represent diastolic (caudocranial) CSF flow. The waveform amplitude was measured from the maximum systolic (MSF) to the maximum diastolic (MDF) CSF flow

arterial and the CSF waveform amplitudes and the negative relationship between the venous and the CSF waveform amplitudes observed in this study support these assumptions. Furthermore, the multiple regression analysis reveals that the cerebral arterial and the jugular venous pulsation amplitudes contribute independently to the CSF pulsation amplitudes and explain a significant proportion of the variance.

The AV delay measured between the maximum systolic slopes of the arterial and venous waveforms did not contribute significantly to predicting the CSF waveform amplitude. The AV delay represents a period during which maximum inflow of the arterial blood has occurred but the maximum outflow of the venous outflow has not yet begun, and it is therefore likely to reflect an interval during which the largest expansion in the cerebral blood volume is taking place. Thus, a shorter AV delay may allow a smaller systolic brain expansion than a longer AV delay, and is likely to be associated with a small CSF flow pulsation amplitude [16]. We believe that the weak correlation observed between the AV delay and the CSF flow pulsation amplitudes may confirm this previously suggested hypothesis. Possibly, the coarse temporal resolution of our study limited our ability to estimate the relationship between these two variables. The failure of AV delay to add significantly to the multiple regression analysis model in predicting the CSF pulsation amplitudes indicate that this variable's contribution is not independent. Indeed, we observed a relationship between the length of the AV delay and the venous waveform amplitudes: a short AV delay was usually associated with a large venous amplitude. It is therefore conceivable that AV delay did not add to the contribution made by the venous amplitudes to the CSF amplitudes.

The data presented here support the notion that the forward transmission of the arterial pulsations through the extra- and intracranial arteries and the cerebral arterioles, and the backward transmission of the right atrial pulsations through the internal jugular, intracranial bridging and cortical veins, combine to generate a composite CSF pressure pulse [22–24]. The results further elaborate that with MR flow imaging methods it is feasible to quantitate the individual contributions of the arterial and venous pulsations to the CSF pulsations. Although we measured flow pulsations instead of pressure pulsations, similarities between the CSF pressure and flow waveforms, and the observations that the jugular venous flow waveforms appear to reflect right atrial pressure changes, indicate that the same physiological phenomenon can be observed by the analysis of the CSF and vascular flow pulsations [14].

The wide variation observed in the jugular venous flow pulsation amplitudes among healthy subjects in this study indicates that under normal conditions, the venous influence on the CSF pulsation may vary. These observations seem to have clinical relevance in light of the prior experimental evidence which suggests that the increased arterial and diminished venous contributions to the CSF pulsations correlate with an elevated level of intracranial pressure and increased CSF pulse pressure [17, 22, 25–28]. These experimental studies have shown that when the intracranial pressure is elevated by intraventricular infusion of saline, similarity between the arterial and the CSF pressure waveforms increases but

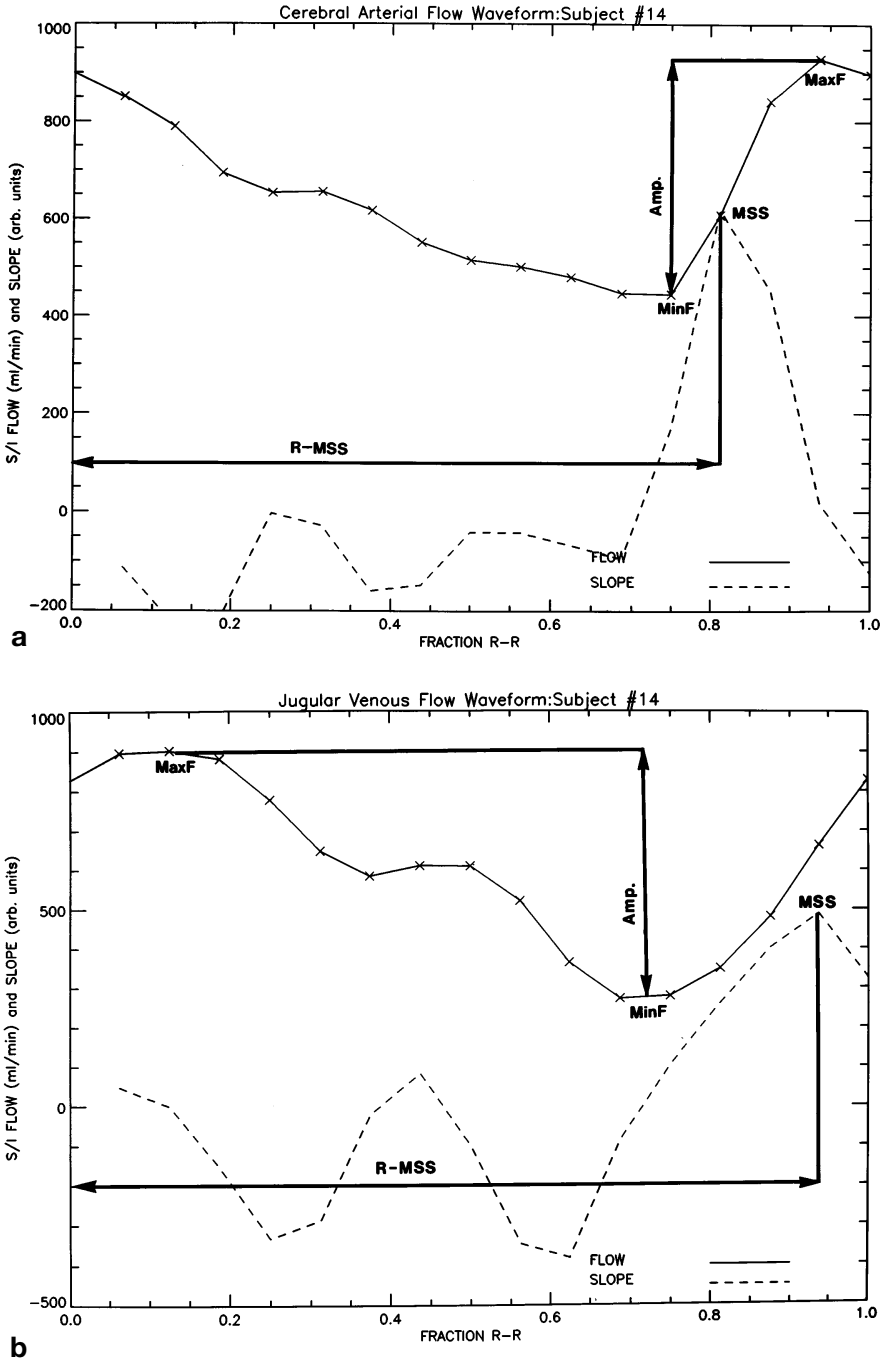

Fig. 3 a, b Cerebral arterial and jugular venous flow waveforms. Fractions of cardiac cycle on X-axis and flow rates in ml/min on Y-axis. The *continuous line* represents flow and the *dotted line* slope. The arterial waveform (**a**) represents combined flow in the internal carotid and vertebral arteries, the venous waveform **b** combined flow in both internal jugular veins. The positive deflections in **a** indicate caudocranial arterial flow and those in **b** craniocaudal venous flow. Vascular waveform amplitudes were measured from maximum (MaxF) to minimum flow (MinF). Arteriovenous (AV) delay was measured by subtracting the R-wave to the maximum systolic slope (R-MSS) interval of the arterial waveform from that of the venous waveforms

that between the CSF and the venous pulse decreases [22, 25, 28]. This is because of a decrease in the impedance on the arterial side and an increase in the impedance on the venous side of the capillary bed [17, 25, 26, 28]. We observed an increase in the CSF flow pulsation amplitude and rounding of its contour (diminished venous contribution) in normal subjects when the venous outflow impedance was increased by jugular venous compression, a maneuver also known to increase the intracranial pressure (unpublished data). Whether the differences in the venous contributions to the CSF flow waveform amplitude indicate that these subjects have different levels of intracranial pressure is a matter which needs further investigation. Since quiet respiration is not likely to affect the flow information by cardiac-gated phase-contrast imaging, and as all of our subjects were breathing quietly [5, 12], it is unlikely that respiratory effects introduced the observed dissimilarities in

Table 1 CSF and vascular waveform amplitudes, R-wave to maximum systolic slope (R-MSS) intervals, and AV delays

	Amplitudes[a]			R-MSS[b]		AV delay[b,c]
	CSF	Arterial	Venous	Arterial	Venous	
Range	95–468	340–860	100–1100	0.82–0.92	0.78–1.16	–0.06–0.27
Average	250.2	529.7	518.7	0.87	0.92	0.05
SD	78.1	144.4	297	0.03	0.08	0.07

[a] ml/min
[b] Fractions of cardiac cycle (temporal values greater than 1 are due to periodicity of the waveforms)
[c] The AV delay is the time between R-MSS of arterial and venous waveforms (negative values indicate that venous R-MSS is shorter than arterial R-MSS)

Table 2 Stepwise forward multiple regression between the dependent variable CSF waveform amplitude and independent variables vascular waveform amplitude and AV delay (Multiple $r = 0.79$, multiple $r^2 = 0.63$, adjusted $r^2 = 0.56$; $n = 21$; F (3,17) = 9.5; significance of model: $p = 0.0006$)

Independent variable	Simple r	Multiple R	Multiple R-square	R-square change	F	P
Arterial amplitude	0.61	0.61	037	0.37	11.2	0.003
Venous amplitude	–0.5	0.77	0.59	0.22	9.7	0.006
AV delay	0.31	0.79	0.63	0.04	1.6	NS (0.15)

the venous waveform amplitudes and its relationship to the CSF waveform amplitudes.

The cardiac cycle-related pulsatile displacement of the brain can also potentially contribute to the intracranial volume compensation achieved by the CSF and vascular displacements [8–10, 15]. We believe that in normal subjects, the inferior displacement of the cervicomedullary region at the foramen magnum may make a very small contribution to the volume compensation achieved by the venous egress and the CSF displacement. Also, an additional sequence with lower velocity encodings than used in this study may have been required to accurately estimate the brain motion [15]. Nevertheless, brain motion may contribute significantly towards compensation of cerebral blood volume variations when an obstruction exists in the CSF pathways. This has been observed in patients with the Chiari I malformation in whom increased cardiac cycle-related brainstem and tonsillar motion have been observed by myelography, intraoperative ultrasound and MRI [29–31].

The quantitative relationship observed between the CSF and the vascular flow pulsations in this study can be further improved by normalizing the waveform amplitudes for the volume of the cranial compartment and by using fast imaging methods with better temporal resolution [32–36]. Although the results have allowed physiological inferences regarding the intracranial dynamics to be made, further studies are required before the clinical applications are contemplated. In this study, we have examined the contributions of the vascular factors to the CSF flow pulsation amplitudes. To ascertain the contributions of the nonvascular determinants of the CSF pulsation amplitudes such as intracranial compliance and the CSF outflow resistance, controlled experimental studies are required [22, 37–40].

Improvement in techniques, and such experiments, may allow use of CSF flow pulsation amplitudes for clinical applications in the non-invasive assessment of cranial dynamics by MRI.

References

1. DuBoulay G, O'Connell J, Currie J, et al (1972) Further investigations on pulsatile movements in the cerebrospinal fluid pathway. Acta Radiol (Diag) 13: 496–523
2. Ohara S, Negai H, Matsumoto T, Banno T (1988) MR imaging of CSF pulsatory flow and its relation to intracranial pressure. J Neurosurg 69: 675–682
3. Levy LM, Di Chiro G (1990) MR phase imaging and cerebrospinal fluid flow in the head and the spine. Neuroradiology 32: 399–400
4. Quencer RM, Post MJD, Hinks RS (1990) Cine MR in the evaluation of normal and abnormal CSF flow: intracranial and intraspinal studies. Neuroradiology 32: 371–391
5. Enzmann DR, Pelc NJ (1991) Normal flow patterns of intracranial and spinal cerebrospinal fluid defined with phase-contrast cine MR imaging. Radiology 178: 467–474
6. Nitz WR, Bradley WG Jr, Watanabe AS, et al (1992) Flow dynamics of cerebrospinal fluid: assessment with phase-contrast velocity MR imaging performed with retrospective cardiac gating. Radiology 183: 395–405

7. Schroth G, Klose U (1992) Cerebrospinal fluid flow. I. Physiology of cardiac-related pulsations. Neuroradiology 35: 1–9
8. Greitz D, Wirestam R, Frank A, Nordell B, Thomsen C, Stahlberg F (1992) Pulsatile brain movement and associated hydrodynamics studied by magnetic resonance phase imaging: the Monro-Kellie doctrine revisited. Neuroradiology 34: 370–380
9. Feinberg DA (1992) Modern concepts of brain motion and cerebrospinal fluid flow. Radiology 185: 630–632
10. Greitz D (1993) Cerebrospinal fluid circulation and associated intracranial dynamics. A radiologic investigation using MR imaging and radionuclide cisternography. Acta Radiologica Suppl 34: 386
11. Henry-Feugeas MC, Idy-Pereti I, Blanchet B, Hassine D, Zannoli G, Schouman-Claeys E (1993) Temporal and spatial assessment of normal cerebrospinal fluid dynamics with MR imaging. Magn Reson Imaging 11: 1107–1118
12. Enzmann DR, Pelc NJ (1993) Cerebrospinal fluid flow measured by phase-contrast cine MR. AJNR 14: 1301–1307
13. Naidich TP, Altman NR, Gonzales-Arias SM (1993) Phase contrast CINE magnetic resonance imaging: normal cerebrospinal fluid oscillation and applications to hydrocephalus. Neurosurg Clin N Am 4: 677–706
14. Bhadelia RA, Bogdan AR, Wolpert SM (1995) Analysis of the cerebrospinal fluid flow waveforms using gated phase contrast MR velocity measurements. AJNR 16: 389–400
15. Enzmann DR, Pelc NJ (1992) Brain motion: measurement with phase-contrast MR imaging. Radiology 185: 653–660
16. Avezaat CJJ, Van Eijndhoven JHM, Wyper DJ (1979) Cerebrospinal fluid pulse pressure and intracranial volume-pressure relationships. J Neurol Neurosurg Psychiatry 42: 687–700
17. Portnoy HD, Chopp M (1981) Cerebrospinal fluid pulse waveform analysis during hypercapnia and hypoxia. Neurosurgery 9: 14–27
18. Bhadelia RA, Bogdan AR, Wolpert SM, Lev S, Appignani BA, Heilman CB (1995) Cerebrospinal fluid flow waveforms: analysis in patients with Chiari I malformation by means of gated phase-contrast MR imaging velocity measurements. Radiology 196: 195–202
19. Monro A (1783) Observations on the structure and functions of the nervous system. Creech and Johnson, Edinburgh
20. Kellie G (1824) Appearances observed in the dissection of two individuals; death from cold and congestion of the brain. Trans Med Chir Soc Edin 1: 84
21. White DN, Wilson KC, Curry GR, Stevenson RJ (1979) The limitation of pulsatile flow through the aqueduct of sylvius as a cause of hydrocephalus. J Neuro Sci 42: 11–51
22. Hamer J, Alberti E, Hoyer S, Wiedemann K (1977) Influence of systemic and cerebral vascular factors on the cerebrospinal fluid pulse waves. J Neurosurg 46: 36–45
23. Hamit HF, Beall AC Jr, De Bakey ME (1965) Hemodynamic influences upon brain and cerebrospinal fluid pulsations and pressures. J Trauma 5: 174–184
24. Cardoso ER, Reddy K, Bose D (1988) Effect of subarachnoid hemorrhage on intracranial pulse wave in cats. J Neurosurg 69: 712–718
25. Portnoy HD, Chopp M, Branch C, Shannon B (1982) Cerebrospinal fluid pulse waveform as an indicator of cerebral autoregulation. J Neurosurg 56: 666–678
26. Chopp M, Portnoy HD (1980) Systems analysis of intracranial pressure. J Neurosurg 53: 516–527
27. Cordoso ER, Rowan JO, Galbrath S (1983) Analysis of the cerebrospinal fluid pulse wave in intracranial pressure. J Neurosurg: 817–821
28. Takizawa H, Gabra-Sanders T, Miller JD (1987) Changes in the cerebrospinal fluid pulse wave spectrum associated with raised intracranial pressure. Neurosurgery 20: 355–361
29. Du Boulay GH, Shah S, Currie JC, Logue V (1974) The mechanism of hydromyelia in Chiari type I malformation. Br J Radiol 47: 579–587
30. Oldfield EH, Muraszko K, Shawker TH, Patronas NJ (1994) Pathophysiology of syringomyelia associated with Chiari I malformation of the cerebellar tonsils: implications for diagnosis and treatment. J Neurosurg 80: 3–15
31. Wolpert SM, Bhadelia RA, Bogdan AR, Cohen AR (1994) Chiari I malformations: assessment with phase-contrast velocity MR imaging. AJNR 15: 1299–1308
32. Kohn MI, Tanna NK, Herman GT, et al (1991) Analysis of brain and cerebrospinal fluid volumes with MR imaging. I. Methods, reliability, and validation. Radiology 178: 115–122
33. Blatter DD, Bigler ED, Gale SD, et al (1995) Quantitative volumetric analysis of brain MR: normative database spanning 5 decades of life. AJNR 16: 241–251
34. Frayne R, Rutt BK (1993) Frequency response of retrospectively gated phase-contrast MR imaging: effect of interpolation. JMRI 3: 907–918
35. Maier SE, Hardy CJ, Jolesz FA (1994) Brain and cerebrospinal fluid motion: real-time quantification with M-mode MR imaging. Radiology 193: 477–483
36. Poncelet BP, van Wedeen J, Weisskoff RM, Cohen MS (1992) Brain paranchymal motion: measurement with cine echo-planar MR imaging. Radiology 185: 645–651
37. Sullivan HG, Miller JD, Searle JR (1980) An interpretation of pressure/volume interaction in the craniospinal axis. Neurosurgery 6: 453–462
38. Marmarou A, Shulman K, LaMorgese J (1975) Compartment analysis of compliance and outflow resistance of the craniospinal system. J Neurosurg 43: 523–534
39. Miller JD, Takizawa H, Riper IR (1989) Cerebral pulse pressure waveform and cerebrospinal fluid outflow resistance. In: Gjerris F, Borgesen SE, Sorensen PS (eds) Outflow of cerebrospinal fluid. Munksgaard, Copenhagen, pp 235–246
40. Avezaat CJJ, Van Eijndhoven JHM (1989) Comparison between volume pressure relationship and resistance to outflow of cerebrospinal fluid during cerebral compression in dogs. In: Gjerris F, Borgesen SE, Sorensen PS (eds) Outflow of cerebrospinal fluid. Munksgaard, Copenhagen, pp 167–178